Collaborative project

Project acronym: SNM

Project full title: "**Single Nanometer Manufacturing for beyond CMOS devices**"

Grant agreement no: 318804

Deliverable: D4.3 (“Prototype beam splitting optics/blanker plate chip stack in SEM.”)

Name of the coordinating person: Prof. Dr. Ivo W. Rangelow, Email: ivo.rangelow@tu-ilmenau.de

List of participants:

Participant no.	Participant organisation name	Part. short name	Activity Type	Country
1 (Co)	Technische Universität Ilmenau	**TUIL**	HER	Germany
2	EV Group E. Thallner GmbH	**EVG**	IND; End-user	Austria
3	IMEC	**IMEC**	RES	Belgium
4	Mikrosistemi Ltd	**µS**	SME; End-User	Bulgaria
5	Universität Bayreuth	**UBT**	HER	Germany
6	Technische Universiteit Delft	**TUD**	HER	Netherlands
7	Spanish National Research Council	**CSIC**	RES	Spain
8	IBM Research GmbH	**IBM**	IND; End-user	Switzerland
9	École polytechnique fédérale de Lausanne	**EPFL**	HER	Switzerland
10	SwissLitho AG	**SL**	SME; End-User	Switzerland
11	Oxford Instruments Nanotechnology Tools Ltd	**OINT**	IND; End-user	UK
12	Imperial College London	**IMPERIAL**	HER	UK
13	The Open University	**OU**	HER	UK
14	Oxford Scientific Consultants Ltd	**OSC**	SME	UK
15	VSL Dutch Metrology Institute	**VSL**	IND	Netherlands
16	University of Liverpool	**ULIV**	HER	UK

SNM
Work Package 4
Deliverable: D4.3 (“Prototype beam splitting optics/blanker plate chip stack in SEM.”)

Lead beneficiary number	6	**Nature**	P	**Dissemination level**	PU
Estimated Person-months	32				
Person-months by partner for the Deliverable	TUD 32				
Estimated Delivery Date	31/12/2016	**Delivery Date**	10/02/2017		
Author	• M. Scotuzzi and C.W. Hagen				
Reviewed by:	• WP4 Leader: C.W. Hagen • WPG1 Leader: A. Knoll • Coordinator: Ivo W. Rangelow				
Criteria and Achieved Results	**Criteria**	**Achieved result**			
	Have a Prototype beam splitting optics/blanker plate chip stack mounted in the SEM.	A prototype beam splitting optics chip stack has been mounted in the SEM, and it has been tested. The blanker chip has been fabricated, and is about to be stacked to the beam splitting optics. Tests are planned for the coming 4 weeks. (See also executive summary at the end of the report.)			

Description of the Deliverable	**Executive summary** We developed a multi beam unit (MBU) as an add-on for an SEM that splits the single electron beam into a square array of 25 beams. Additional micro-fabricated optical components were added to focus these beams in a deflector array plane, such that each beam can be blanked individually. A special support assembly was designed and built to allow for stable insertion of the MBU into the SEM and to allow for mechanical alignment to the optical axis of the SEM. The assembly contains electrical feedthroughs for all electrode voltages. The beam splitting optics and the focusing optics was tested successfully, making use of optical imaging of the array of beams falling on a fluorescence screen. The blanker plate was designed and fabricated, and is almost ready to be included in the MBU. Tests will be done shortly, and if successful, the results will be added as an addendum to this report. **Introduction** In Delft we have developed a Multi Beam Scanning Electron Microscope (MB SEM), shown in figure 1, that can enhance the imaging throughput by a factor of 196 [1,2]. The beam is split into 196 beams in the source module and further accelerated into the Coulomb Tube. In this design, the original source module is replaced with a homemade source module, which consists of a filament, an extractor, a suppressor, a set of three-electrodes, a multi beam aperture array and an accelerator lens. In this multi beam source module, individual beam blanking is not implemented. Though attempts were made in the past to introduce a deflector array in the source module, the difficult boundary conditions of ultra-high vacuum, high tension and the large number of feedthroughs (196 driving signals plus the common ground), made it a really challenging task. After careful considerations, we decided to design a new concept of a multi beam SEM.

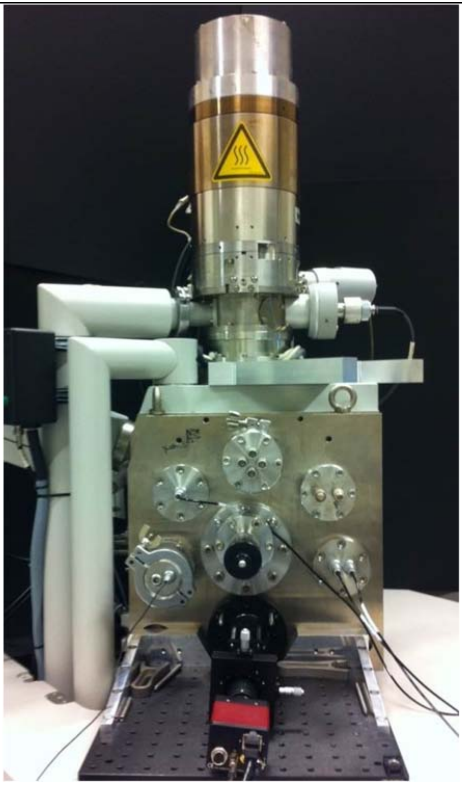

Fig. 1 The Multi Beam Scanning Electron Microscope (MBSEM) with 196 beams.

Figure 2 shows the schematics of the optics of a scanning electron microscope in single beam mode. The beam is generated in the source module and the source is imaged by a set of lenses on the sample surface. Roughly in the middle of the optics, a variable aperture is positioned, to limit the current of the beam. In such configuration, an easier way to split the beam would be to place a multi beam unit (MBU) in the variable aperture position. The multi beam unit can be easily inserted in the variable aperture port of a scanning electron microscope, providing *flexibility* and *versatility*, namely the changes to be made to a standard microscope do not have to be permanent and will fit easily in a variety of SEM's. The beam splitting optics consists of a combination of a deceleration lens, a macro lens and a micro-lens aperture array. To enable individual blanking of each beam for e-beam lithography or Electron Beam Induced Deposition, a deflector array is also installed, below the beam splitting optics. The schematics in Figure 3 show the optical design of an SEM with a multi beam unit (MBU). In this system, the source is imaged by the C1 and C2 lenses in a plane above the Multi Beam Unit, which is represented by the red dashed line. The primary beam is split into beamlets by means of the Micro Lens Array (MLA) and focused in the blanker plane (or deflector array plane). All beamlets have a common crossover in the coma-free plane of the objective lens (UHR) and are focused in the sample plane.

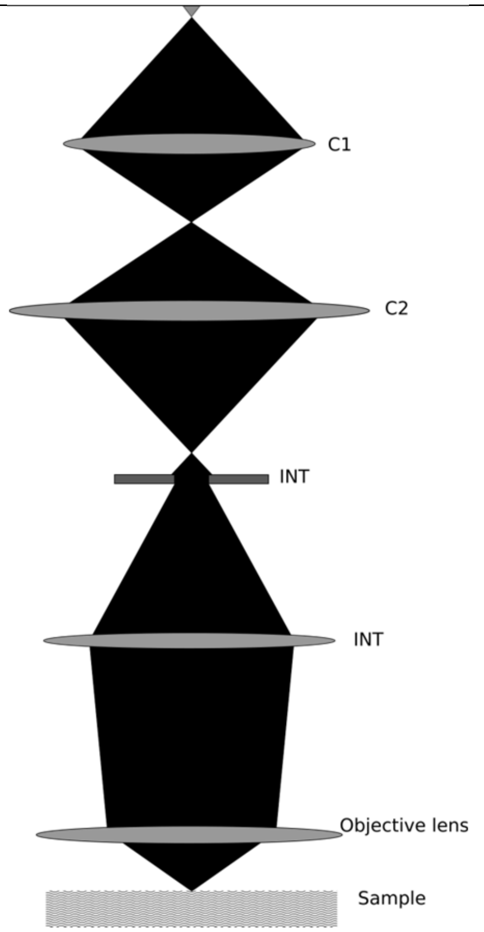

Fig. 2 Optical schematics of an electron microscope in single beam mode

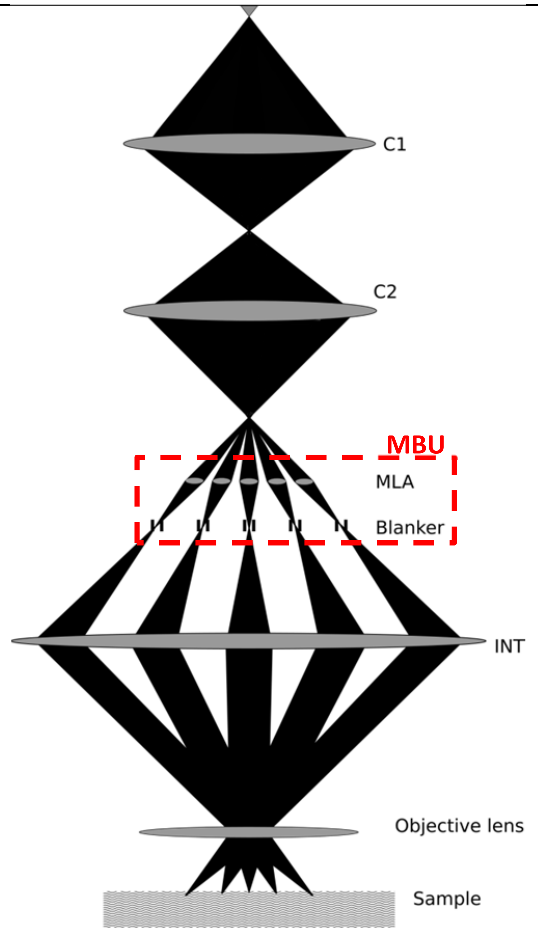

Fig. 3 Optical schematics of an electron microscope in multi beam mode

The MLA and the blanker plate need to be designed such that they fit in the Variable Aperture port, which has a circular shape of 1 cm in diameter. Moreover, to obtain the lens effect on the MLA and the possibility to compensate for field curvature of the outer beams, at least two electrodes need to be added above the MLA plate. The entire chip stack must then be enclosed into a grounded cylindrical shielding.

In the MS7 report several optical designs were presented, but there was still some freedom of choice for the micro-lens size and pitch. For the final design we chose a micro lens diameter of 5 µm. The optimal parameters, found by minimizing the probe size at the sample, are summarized in Table 1.

Diameter of MLA aperture	5 µm
Distance between MLA and blanker plate	4 mm
Working distance (distance between the objective lens and the sample)	3 mm
Acceleration voltage	5 kV

Table 1 Optimal parameters of the Multi Beam Blanker Unit geometry.

Figure 4 shows a cross-section of the Multi Beam Blanker Unit. Three macro electrodes (D, E1 and E2) are positioned above the beam splitting plate. D decelerates the beam to an energy of 3.5 kV, E1 forms a zero strength lens which can correct for the field curvature and E2 provides the electric field on the MLA, to form the lens effect on the apertures. The MLA is positioned below E2 and 4 mm above the blanker plate. Insulating spacers will be positioned in between electrodes, while a rigid support holds the blanker plate and the stack of electrodes consisting of D, E1, E2 and the MLA.

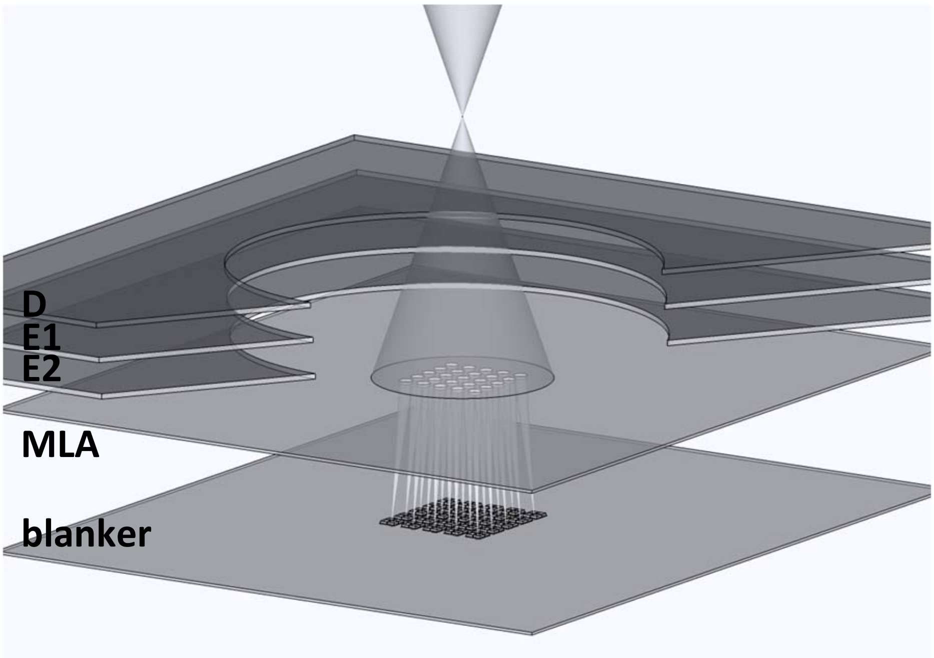

Fig. 4 Cross-section of the Multi Beam Blanker Unit

To characterize this system by its optical properties the on-axis aberrations must be evaluated. On-axis aberrations include diffraction, spherical aberration and chromatic aberrations. The contributions to the total probe size can be calculated using the following equations 1-5 [3]:

1. *Source image*

$d_{geo} = d_{source} \cdot M$,

where d_{source} is the virtual source size, and M the magnification

2. *Diffraction*

$d_{diff} = 0.54 \cdot \frac{\lambda}{\alpha} = 0.54 \cdot \frac{1.266 \cdot 10^{-9}}{\sqrt{V} \cdot \alpha}$ [m],

Where λ is the wavelength, V is the acceleration voltage (in V) and α the half opening angle

3. *Spherical aberration*

$d_{sph} = 0.18 \cdot C_s \cdot \alpha^3$,

where C_S (the spherical aberration coefficient) is calculated according to the type of lens:

- Magnetic Lens: $C_s = \frac{0.24 \cdot f^3}{S^2 + 0.45 \cdot d^2}$
- Electrostatic Lens: $C_s = \frac{f^3}{d^2}$
- Single electrode lens: $C_s = \frac{f^2}{d}$

where f is the focal distance, d the lens diameter and S the lens gap.

4. *Chromatic aberration*

$d_{ch} = 0.6 \cdot C_c \cdot \frac{\delta U}{V} \cdot \alpha$

where C_C (the chromatic aberration coefficient) is taken equal to f and δU is the energy spread in the beam.

The final probe size is calculated according to the following equation:

$$d_{probe} = \left(\left(\left(d_{geo}^{1.3} + \left(\left(d_{diff}^4 + d_{sph}^4 \right)^{\frac{1}{4}} \right)^{1.3} \right)^{\frac{1}{1.3}} \right)^2 + d_{ch}^2 \right)^{\frac{1}{2}}$$

Figure 5 shows the variation of the total probe size and the on-axis contributions at the sample as a function of the half opening angle of the beam at the sample. The smallest achievable probe size delivering 50 pA at the sample is 1.5 nm, corresponding to a half opening angle of 14.59 mrad. The pitch at the wafer is 0.4µm.

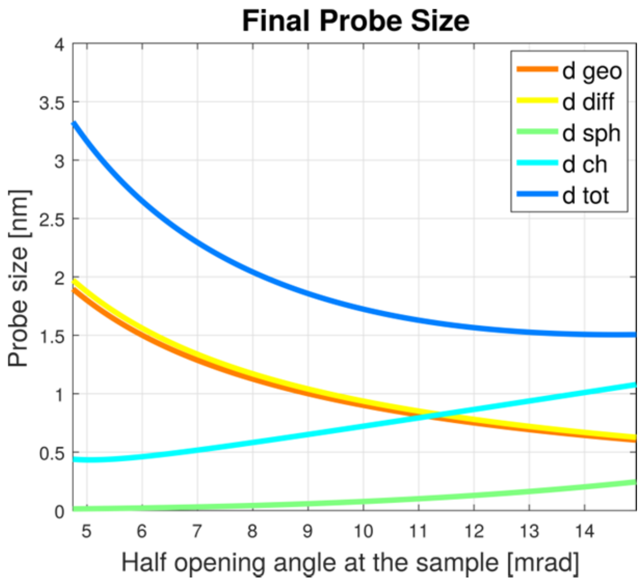

Fig. 5 Variation of the total axial probe size and the on-axis aberration contributions to the probe as a function of the beam half opening angle at the sample

Off axis aberrations are also evaluated. The contributions to the probe size are:

- Astigmatism: $d_{AS}(i,j) = M \cdot \sqrt{2} \cdot h^2(i,j) \cdot \alpha \cdot \sqrt{C_a^2 + c_a^2}$
- Field Curvature: $d_{FC}(i,j) = M \cdot \sqrt{2} \cdot h^2(i,j) \cdot \alpha \cdot |D_a + C_a|$
- Coma: $d_{CO}(i,j) = M \cdot \sqrt{2} \cdot h(i,j) \cdot \alpha^2 \cdot \sqrt{F_a^2 + f_a^2}$
- Chromatic Aberration: $d_{CH}(i,j) = M \cdot \sqrt{2} \cdot h(i,j) \cdot \frac{\Delta U_{50}}{U} \cdot \sqrt{C_{Da}^2 + c_{\Theta a}^2}$
- Total contribution off axis:

$$d_{off-axis-tot}(i,j) = \sqrt{d_{AS}(i,j)^2 + d_{FC}(i,j)^2 + d_{CO}(i,j)^2 + d_{CH}(i,j)^2}$$

Total contribution to the probe size: $d_{tot}(i,j) = \sqrt{d_{axial}^2(i,j) + d_{offaxis}^2(i,j)}$

Where α is the half opening angle of the beam, M the magnification of the lens shown in figure 6a. h is the distance of the off-axis microlens to the center of the MLA, as depicted in Figure 6b. C_a, c_a, D_a, F_a, f_a, C_{Da} and $C_{\theta a}$ are the off-axis aberrations coefficients for astigmatism, field curvature, coma and chromatic aberrations. These coefficients are calculated by simulating the actual lenses with a finite element simulation package (EOD by SPOC, Brno). Because the beamlets in the C1 and C2 lens come from an object on the optical axis, the off-axis contribution of these lenses can be neglected.

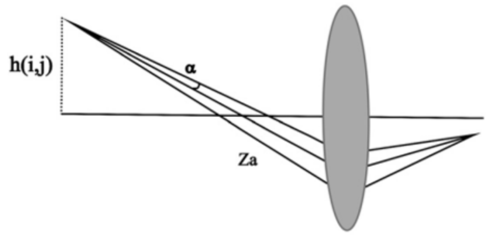

Fig. 6a Off axis beam focused on the image plane by a lens

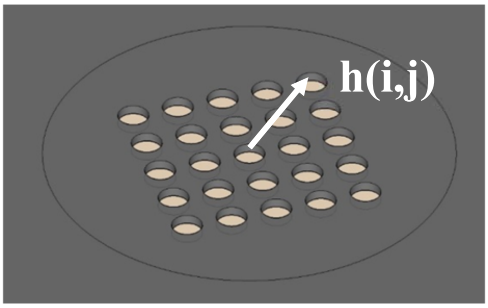

Fig. 6b Height of the aperture on the MLA

Figure 7 shows the off axis contributions to the probe size at the sample for different half opening angles of the beamlet at the sample. For small opening angles, the probe size is strongly limited by the field curvature, which can be minimized by the zero strength lens. The minimum probe size is given at 14 mrad half opening angle that gives a total probe size of approximately 1.6 nm, as shown in figure 8.

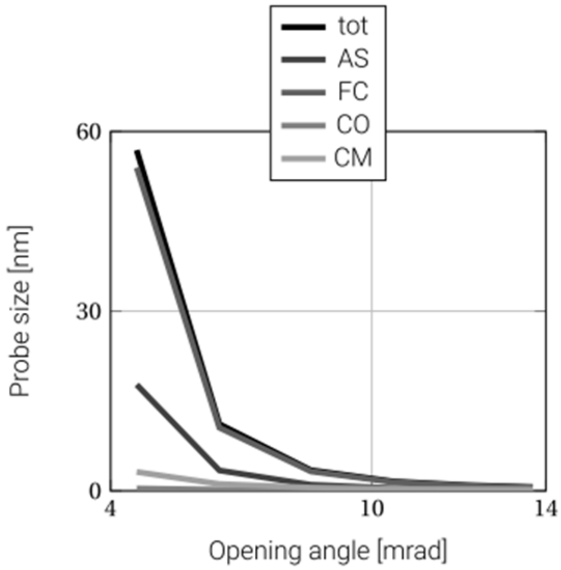

Fig. 7 Off axis contributions to the probe size and total probe size at the sample for different half opening angles of the beams at the sample.

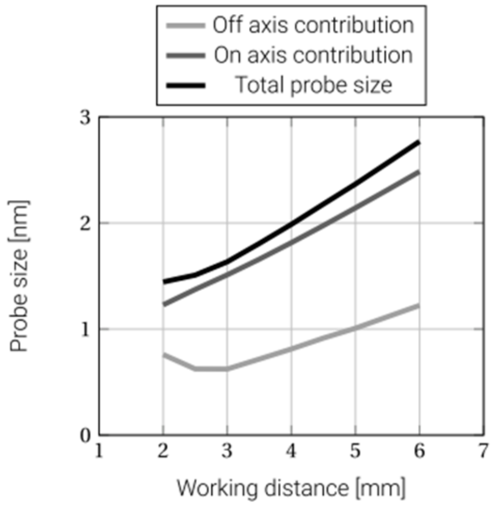

Fig. 8 On-axis and off-axis contributions to the probe size and total probe size at the sample for different working distances.

Also Coulomb Interactions are evaluated, for trajectory displacement and energy spread. The system is split into segments and for each of these segments the Coulomb interactions are calculated, as shown in figure 9. Segments S1, S2 and S3 can be calculated using the usual rules of thumb ([4], see also MS7 report). However, this is not the case for segments S4 and S5 because the beam is split into beamlets below the MLA, which overlap for most of the path. Therefore, a pessimistic approximation is introduced: we consider only the central beam with a current equal to 25 times its own current (50 pA), as if all the beams would perfectly overlap from the MLA down to the sample.

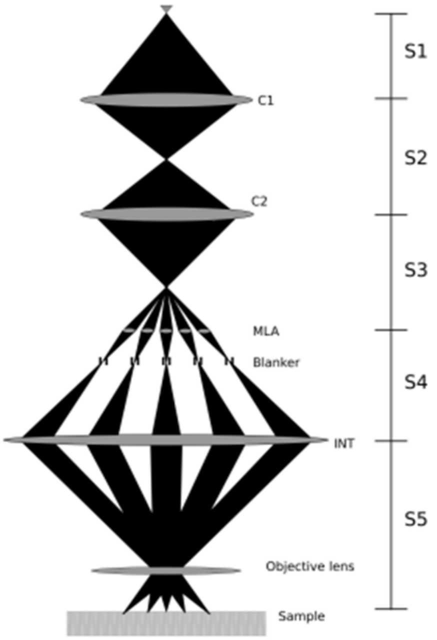

Fig. 9 The optical column is divided into five segments for which the statistical Coulomb interactions are calculated.

Though this is a very pessimistic approximation, the trajectory displacement, as depicted in figure 10, remains below 1 nm, and the Boersch effect (the energy spread), as shown in figure 11, stays within 10 meV (the curves for the S2 and S3 sections saturate because of an angle-limiting aperture in the C2 lens). So, the statistical Coulomb interactions do not pose a problem.

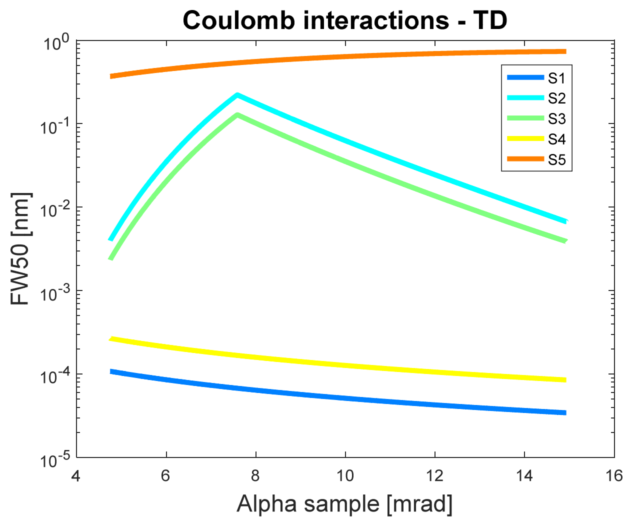

Fig. 10 Probe size contribution due to trajectory displacement.

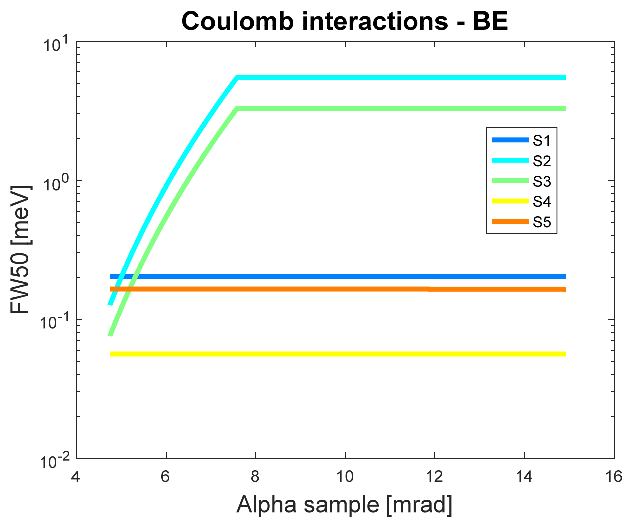

Fig. 11 The Full-width containing 50% of the energy distribution due to the Boersch effect.

In the chosen configuration, the total beam size at the MLA is 66.65 µm in diameter. Considering that each aperture in the MLA has a diameter of 5 µm and they are positioned at a pitch of 7.5 µm, the total beam can be split into 49 beams. However, to be able to cover a large area, i.e. patterning in multiple steps, it is more convenient to split the beam into a square array of beamlets. In this case the total number of beamlets is 25. Because of the inclination of the beamlets, the pitch at the blanker plate is bigger than that at the MLA and is approximately 8.56 µm. The pitch between beams is chosen such that there is enough space for the wiring of the blanking electrodes. Figure 12 shows the design of the blanker plate and the deflector electrodes. The diameter of the 25 holes on the blanker plate is approximately 2.5 µm, which is also the distance between the deflector electrodes. The length of the electrodes is 4 µm, their width is 2.5 µm and their height 2 µm. In such a configuration there is limited space for in-plane wiring, and multiple layer designs are required. However, this complicates the fabrication process considerably and requires also more time. Therefore we decided to fabricate only 3 deflectors, positioned on the diagonal of the array, starting from the central one, as depicted in Figure 13. In addition, a macro deflector is positioned outside of the blanker array area. The idea is to deflect all beams together with the macro deflector and bring back one of the beams by activating its micro deflector electrodes.

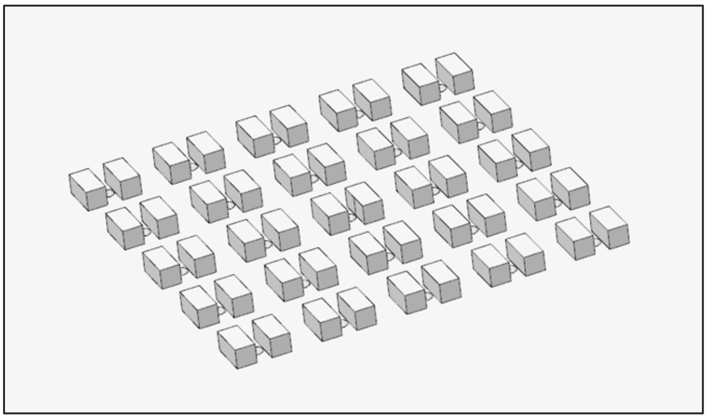

Fig. 12 Design of the deflector electrodes on the blanker plate

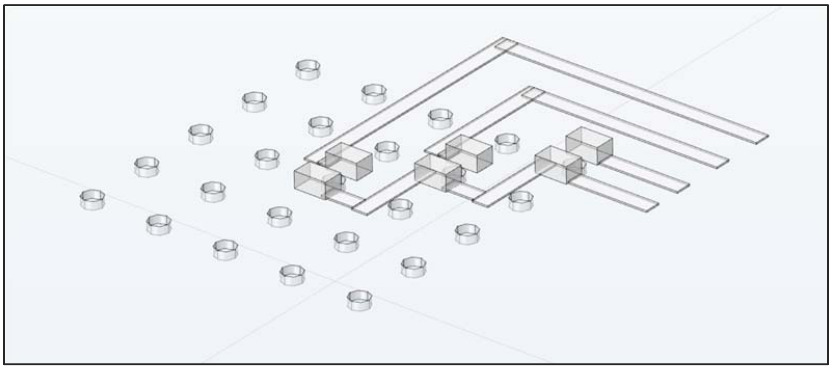

Fig. 13 Design of the deflector electrodes on the blanker plate, in the prototype configuration with 3 micro electrodes only.

Funded by
the European Union

Optics simulation

Figure 14 shows the optical design geometry with the grounded shielding on both ends of the stack, a decelerating lens electrode , two lens electrodes E1 and E2, and the MLA. The voltages on the electrodes are: shielding and MLA at GND potential, decelerating lens electrode at -1.5 kV, E1 at +1 kV, and E2 at +4.8 kV.

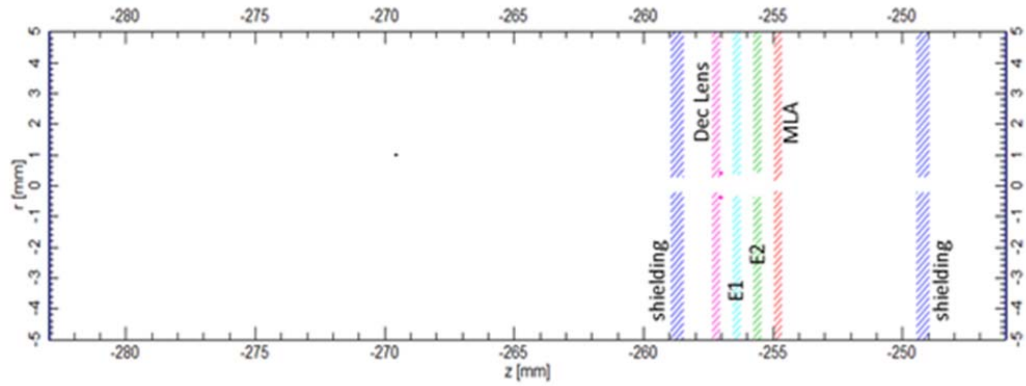

Fig. 14 The electrode geometry of the beam splitting optics stack.

In figure 15 the electrostatic fields are shown as calculated from a finite element package (EOD by SPOC, Brno), and ray traces are shown for the central beam. It is seen that the rays focus at 4 mm distance from the MLA. This is the position where the deflector plate (blanker plane) will be placed.

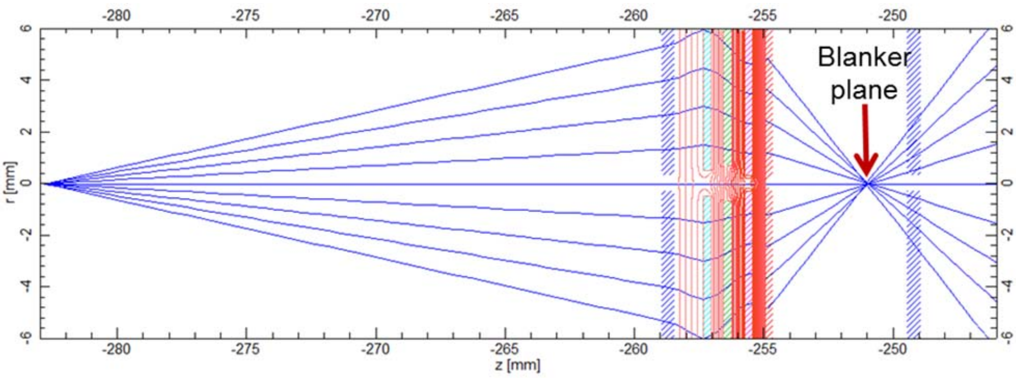

Fig. 15 The equipotential lines of the calculated fields are shown in red between the electrodes, and the ray traces are shown in blue (not at the same scale as the geometry).

Fabrication process

The MLA and the macro electrodes were fabricated using microfabrication techniques in the Kavli-nanofacility in Delft. A set of Masks was designed for the lithography process for the fabrication of the macro electrodes and the MLA plate. Markers were included in the masks to facilitate alignment in the stacking process of the electrodes. The process steps of the MLA fabrication are sketched in Figure 16.

We used a SOI wafer, i.e. Silicon on Insulator with an oxide layer buried below the upper Silicon layer, and deposited oxide on both sides using PECVD. First, the aperture array geometry is patterned in the photoresist, spun on the top side, using optical lithography. Subsequently, etching steps open up the upper oxide layer and the Si device layer, stopping on the buried oxide layer. Then, on the other side of the wafer, called the handle, the back hole is patterned in the photoresist with a second optical lithography step. The backside hole is etched into the oxide layer, and then after resist stripping into the Si handle. Finally the buried oxide layer is removed, leaving a thin Si membrane, with a thickness equal to that of the device layer.

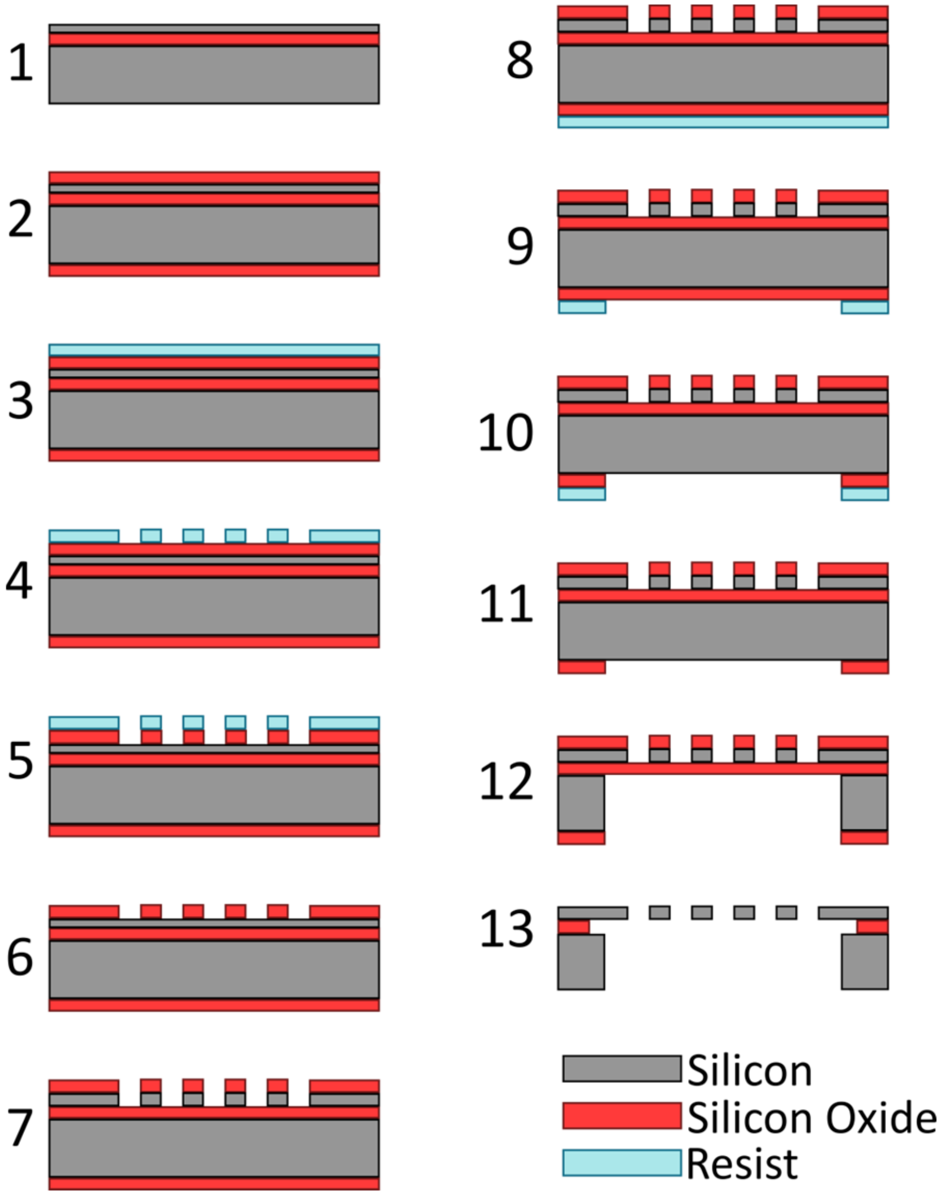

Fig. 16 Schematic overview of the process steps in the fabrication of the Micro Lens Array (MLA).

The device layer of the SOI wafer, used for the fabrication of the MLA, has a resistivity of ~50 µΩ.cm, so no full metallization was needed. The macro-electrodes were made out of a 300 µm thick Si wafer, with a device layer of 10 µm. Only one end of the MLA electrode and the macro-electrodes was metallized with Al to enable wire bonding to nearby contact pads. An example of the MLA is shown in Figure 17.

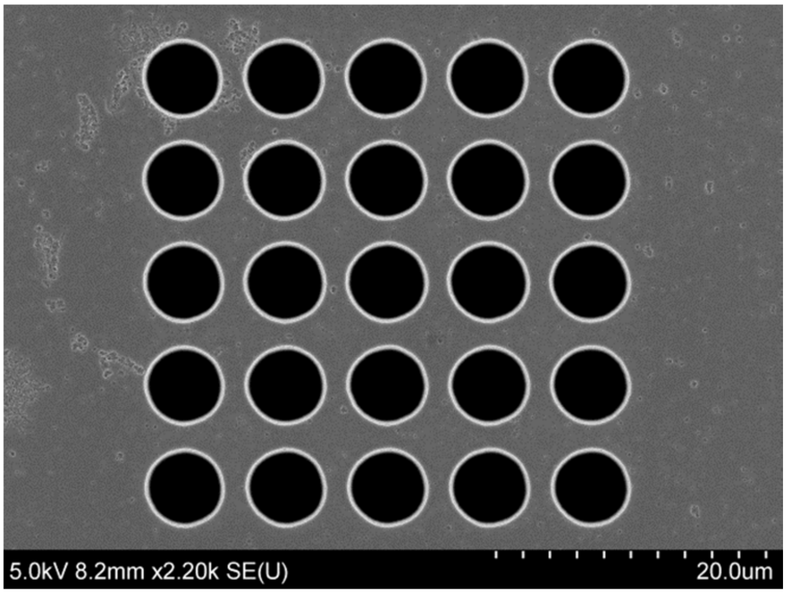

Fig 17 An SEM image of the MLA. It consists of 25 aperture lenses of 5 µm radius at a 7.5 µm pitch etched out of a 10 µm thick Si membrane.

To stack and align the macro-electrodes and the MLA we used a specially developed alignment tool based on a 6-degrees of freedom PI-hexapod system. This system has a proven alignment accuracy of 500 nm [5]. The alignment tool is shown in figure 18.

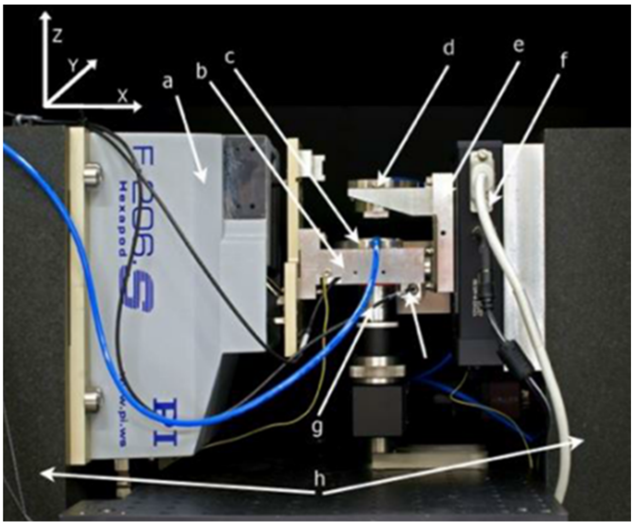

Fig. 18 The 6D-alignment tool. a) the 6D-stage (PI F206 hexapod), b) 6D-stage mounting fork, c) lower element chuck, d) upper element chuck, e) z-stage mounting fork, f) z-stage (PI M605-1D), g) microscope objective, h) granite stage mounting blocks.

The macro-electrodes are electrically separated from each other by double layers of glass spacers, to reduce the risk of voltage breakdown and flashover. All electrodes were fixed by gluing them together using UV-hardening glue. Figure 19 shows an SEM image of the beam splitting optics stack. For the first test of the beam splitting optics we decided not to include the deflector plate yet.

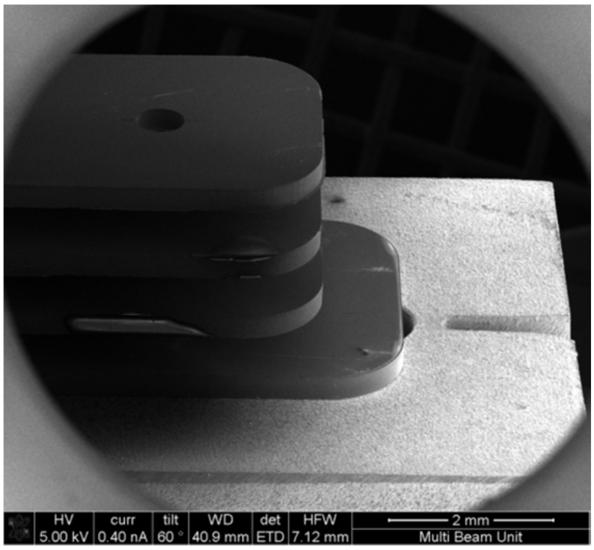

Fig. 19 An SEM image of the beam splitting optics stack, consisting of 3 macro-electrodes (on top) and the MLA (bottom).

Electrical contacts were brought close to the electrode stack using specially designed flexible prints. This is seen in figure 20 (left). In figure 20 (right) an SEM image is shown of the wire bonds connecting the electrodes to the flex print.

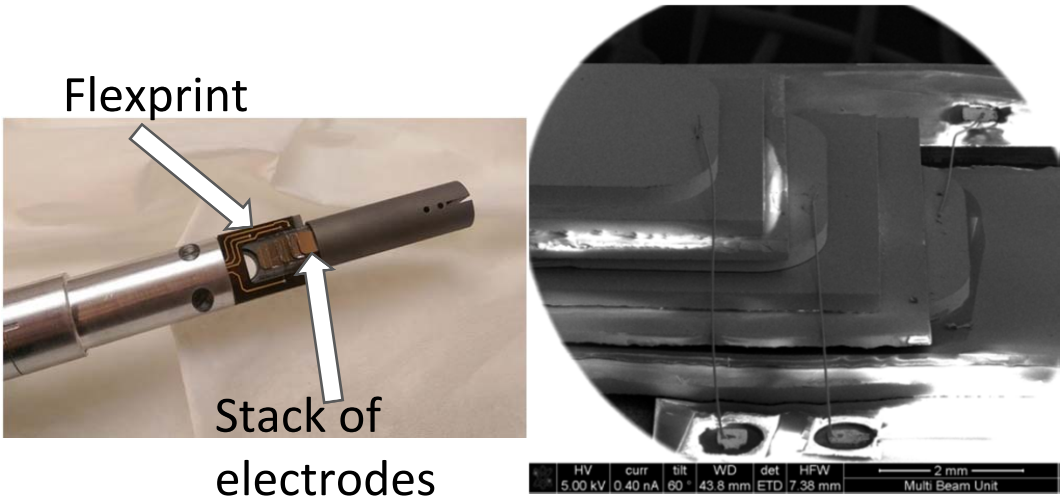

Fig. 20 Left: part of the flex print is seen next to the rear of the electrode stack. Right: SEM image of the wire bonds between the electrode stack and the contact pads of the flex print.

Mechanical design of the support apparatus

The stack has to be inserted in the electron optical column of the SEM, and it needs electrical feedthroughs. Therefore it cannot be mounted on the standard variable aperture holder and a new holder was designed and built. There are a number of requirements to fulfil. First, the size of the chip stack support that sticks into the column has to fit into a 10 mm diameter circular hole in the column wall. Within this size also all wiring needs to fit. For the prototype we chose to simplify the design such that all relevant tests can be done. This means that we chose not to control the blanking of each of the 25 beams, but of three beams only: the central beam, and the next two beams along a diagonal of the square array. This will give us sufficient information on the proper working of the device. This reduces the number of feedthroughs considerably, such that we can wire all electrodes directly, without having to consider multiplexing electrode voltages. All materials used for the mechanical support have to be non-magnetic and parts visible to the electron beams need to be electrically conducting. In addition all materials need to be vacuum compatible down to a vacuum of 10^{-6} mbar. Titanium and phosphor bronze were used for the fabrication of the support. The chip stack will contain the multibeam splitting array as well as a conventional single aperture, to allow for single beam operation. This requires movement of the chip support to position the single aperture under the electron beam. To align the aperture, as well as the multibeam splitting array, to the optical axis of the SEM, displacement in the lateral XY plane (see figure 21) is required. The stroke in Y is 2.5 mm (the distance between the single beam aperture position and the multi beam aperture array position) the range in Y is ±0.5mm. The displacement accuracy in X and Y is 5µm. Furthermore rotation around the support axis is required, as well as tilt, to position the chip stack perpendicular to the optical axis, with an accuracy of 3 mrad. The tilt has its pivot point (P in figure 21) not on the optical axis but near the column wall. Therefore tilts have to be slightly compensated by a translation.

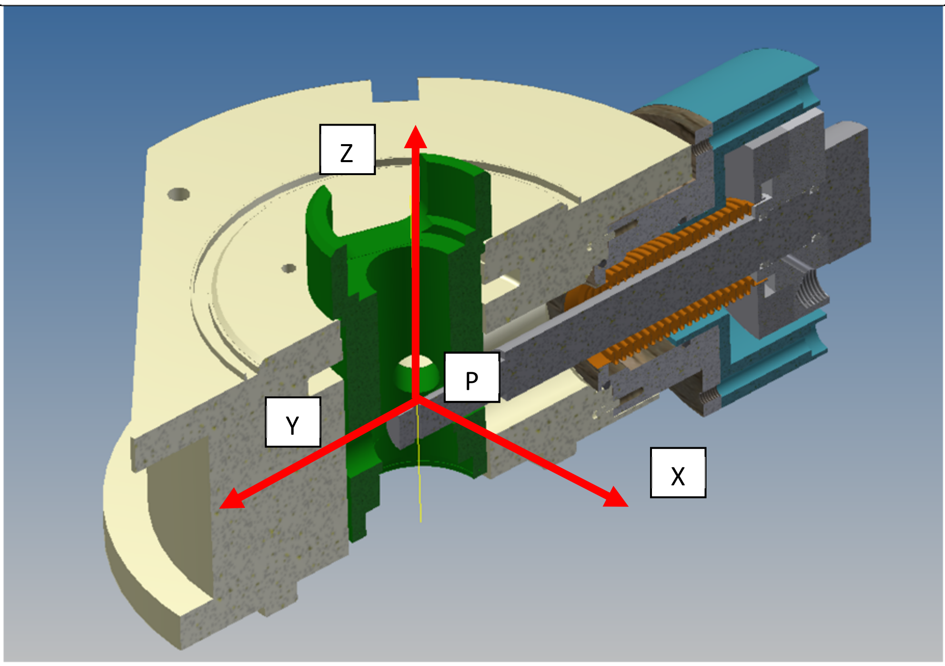

Fig. 21 Definition of the axis system

The entire construction has to be vacuum tight and mechanically stiff, to guarantee a stable position of the aperture array with respect to the optical axis.

The chip stack support assembly is shown in Figure 22a. Figure 22b shows the schematic drawing of the chip stack support, figure 22c shows a schematic drawing of how the assembly is attached to the microscope, and in figure 22d the actual fabricated assembly is shown, mounted to a test part resembling the electron beam column.

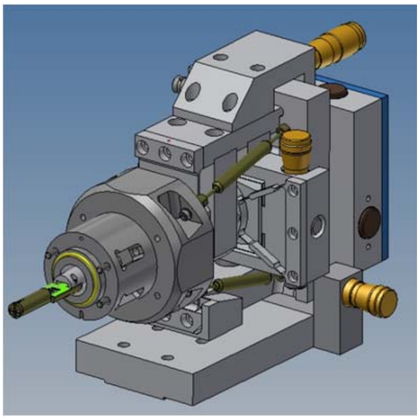

Fig. 22a A schematical drawing of the chip stack support assembly.

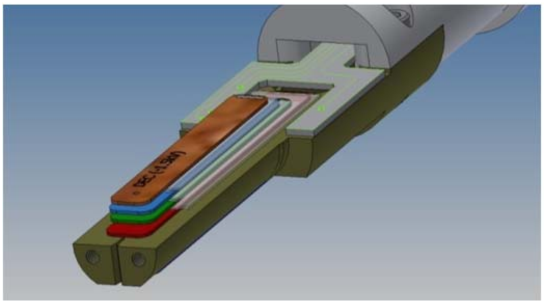

Fig. 22b Schematical drawing of the support with the chip stack mounted on top.

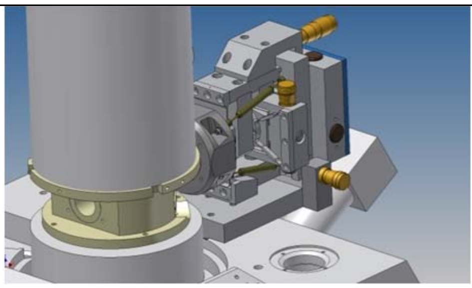

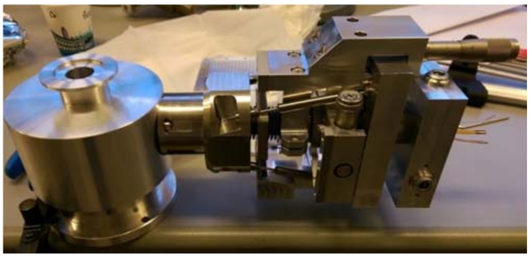

Fig. 22c Schematical drawing of the assembly mounted to the SEM column.

Fig. 22d The assembly mounted to a test part resembling the SEM column.

Figure 23 shows the assembly attached to the FEI NovaNanoLab SEM.

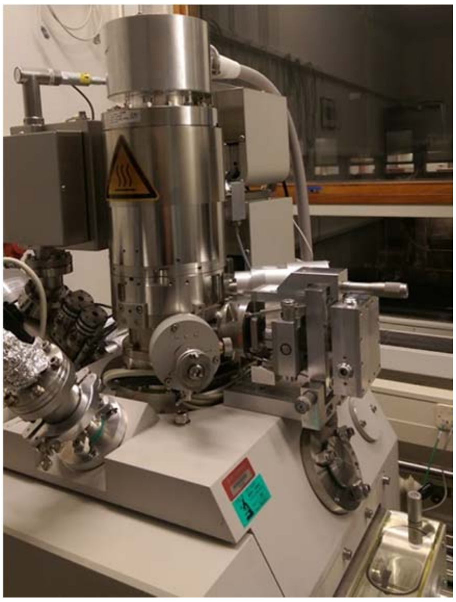

Fig. 23 The chip stack support assembly mounted to the FEI NovaNanoLab SEM.

Experimental results

The first tests were done with just the beam splitting optics stack mounted. Figure 24 shows a shadow image of the MLA, obtained by grounding all the macro electrodes and the MLA plate. The shadow image is obtained by effectively defocusing the beam at the sample.

Lens settings		
MBBU	Dec	0V
	E1	0V
	E2	0V
Microscope	C1	1306V
	C2	
	INT	0
	HR	1.775
	UHR	1

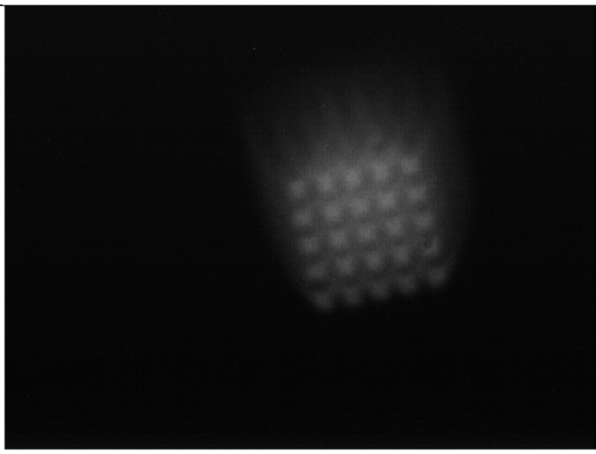

Fig. 24 Shadow image of the MLA for the lens settings shown on the left.

We then imaged the MLA in the so-called cross-over mode of the microscope This is done by focusing the C2 cross-over on the MLA plane and reducing the scan field by decreasing the deflection range of the gun shift coils. There is some contamination seen in the central aperture (see figure 25).

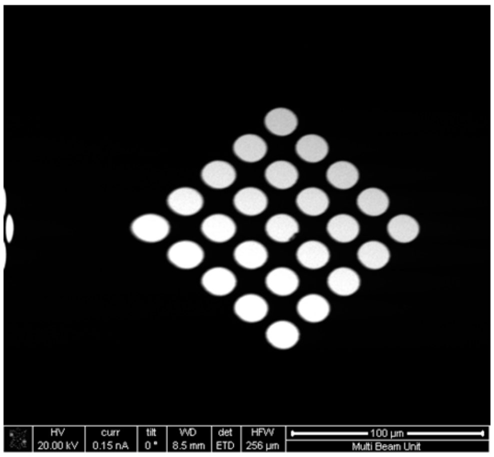

Fig. 25 Cross-over mode image of the MLA, detected using the Everhart Thornly Detector, the standard SE-detector.

To test the focusing optics of the stack we need an image of the focused beam spots in the sample plane. For that we mounted a SECOM platform (6) in the SEM (see figure 26), which provides us with an optical microscope that views samples from underneath. As a sample we mounted a YAG screen (a fluorescence screen) such that we can record a light optical image of the 25 beams simultaneously.

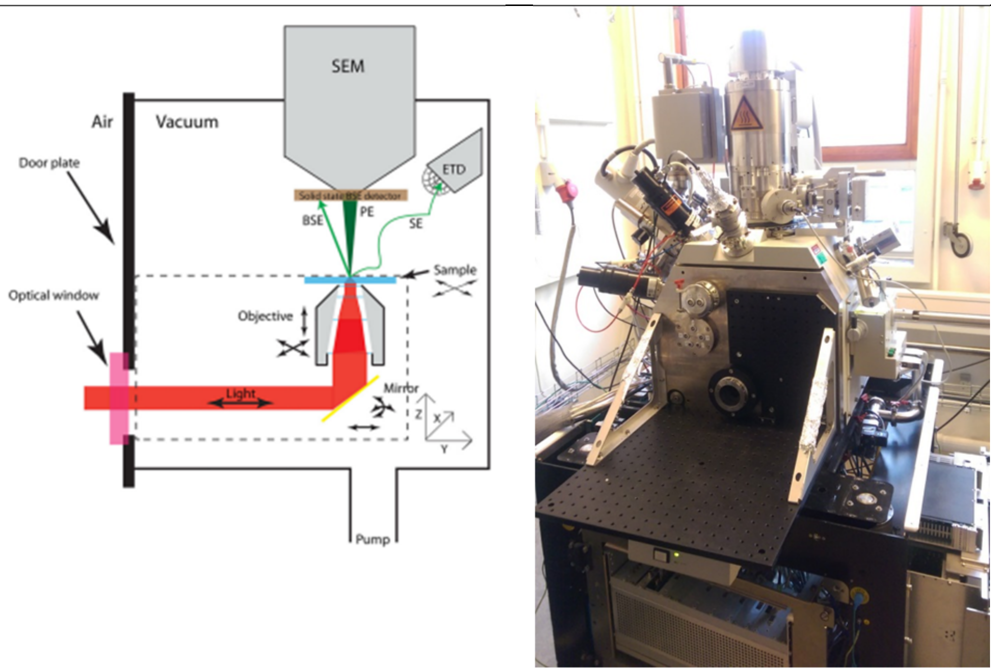

Fig. 26 Left: schematic of the SECOM platform mounted in an SEM. Right: View at the SECOM platform moiunted in the SEM. Also seen is the chip stack assembly mounted in the variable aperture port on the lower right side of the column.

To image the YAG screen onto a camera, we used a 10x objective with a 200mm tube lens. A Guppy camera with 7.4 µm pixel size was used, so effectively we obtain an image with a 740 nm pixel size. This is not sufficient, of course to judge the spot size, but it is sufficient to judge the focusing capability of the chip stack.

In the table below the settings of the lenses are listed for the image shown in figure 27. It clearly shows 25 focused beams, having the smallest possible size that could be obtained by going through focus.

Lens settings		
MBBU	Dec	180V
	E1	-400V
	E2	-1840V
Microscope	C1	1467V
	C2	0.516
	INT	3.798
	HR	0.17
	UHR	1.5839

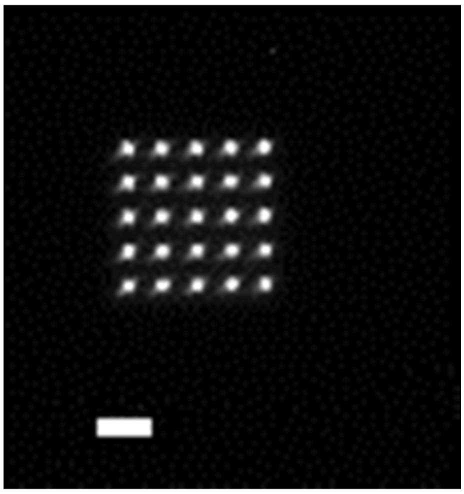

Fig. 27 Optical image of the 25 beams focused on a YAG screen. The scale bar is 10 µm.

Further experiments are underway to optimize the lens settings for the smallest probes. In fact, judging the probe size is a lot easier with the blanker plate installed, because then we can blank all beams but one, and make an image with that beam. From the details in the image a good estimate of the spotsize is obtained. Below we describe the fabrication process of the blanker plate, and simulations of the deflection angles. We start with the simulations.

Deflection angle simulations of the blanker plate

The geometry of the prototype blanker plate was already shown in figure 13. And from figure 15 it is clear that the beam splitting optics focuses the beams at 4 mm distance from the MLA. This is where the blanker plate is to be installed. Figure 28 shows a top view of the prototype design of the blanker plate.

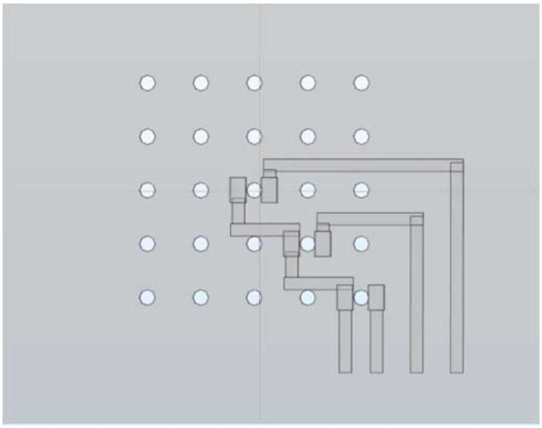

Fig. 28 Top view of the three micro deflectors. The distance between the electrodes is 2.5µm, and the width of the connecting leads is 2 µm.

For reasons described on page 12, two macro electrodes were designed outside of the array of micro deflectors. The effect of the micro and macro deflectors was simulated using COMSOL. The geometry is shown in figure 29.

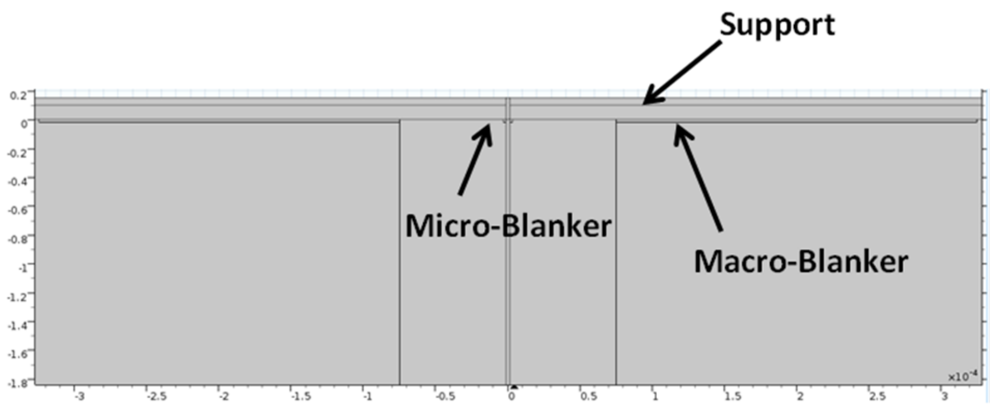

Fig. 29 COMSOL geometry to simulate the deflection angles of the micro and macro deflectors.

The electric fields are calculated in COMSOL In figure 30 the equi-field strength lines are plotted. It is then possible to calculate the particle trajectories of all beams in different situations (micro-deflectors ON/OFF and macro-deflectors ON/OFF). A simulation of trajectories due to the macro deflector only is shown in figure 31. The macro deflector will deflect all the beams such that they can be stopped at an aperture in the plane of the UHR lens.

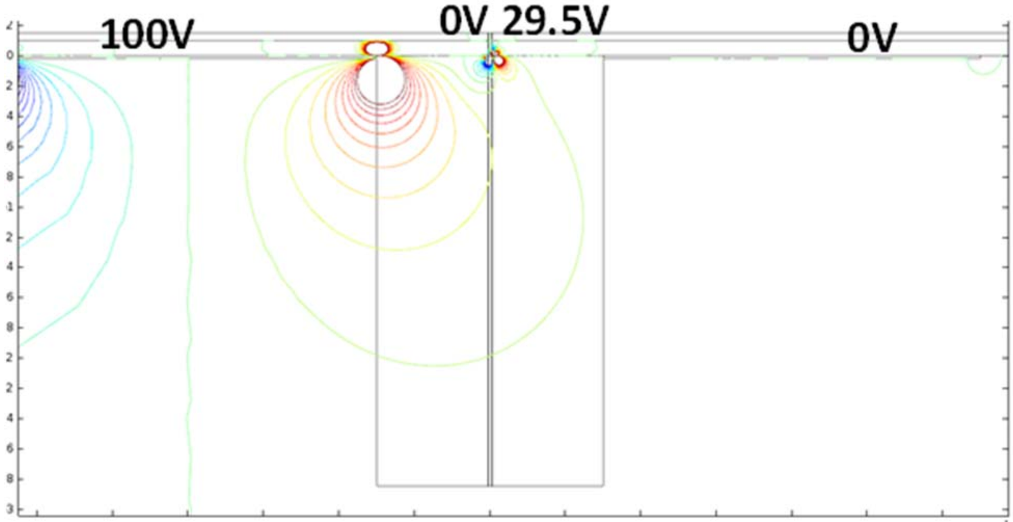

Fig. 30 COMSOL simulation of the electrostatic fields due to the indicated voltages on the micro and macro deflectors. The equi-field strength lines are shown

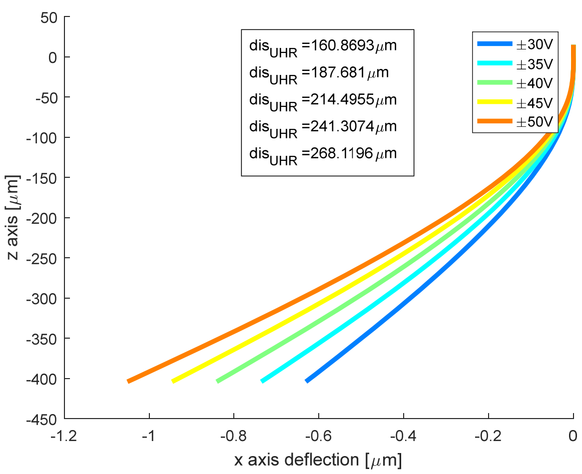

Fig. 31 The deflection as a function of the distance towards the macro deflector, located at z=0. The displacement of the trajectories in the UHR lens plane are indicated in the inset for the indicated voltages ranging from 30-50 V, applied symmetrically to both electrodes.

Figure 32 shows that the displacement varies linearly with the voltage on the macro deflector. Similar simulations of the effect of the micro deflectors are shown in figures 33 and 34.

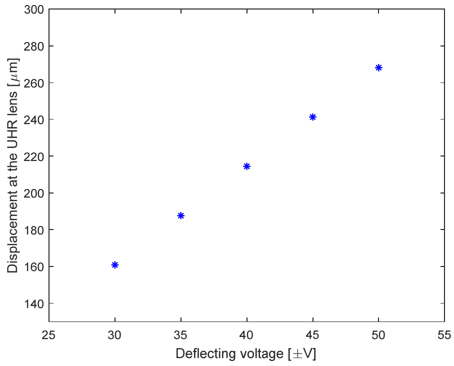

Fig. 32 Deflection of the central beam when the macro blanker is active with the indicated deflecting voltages.

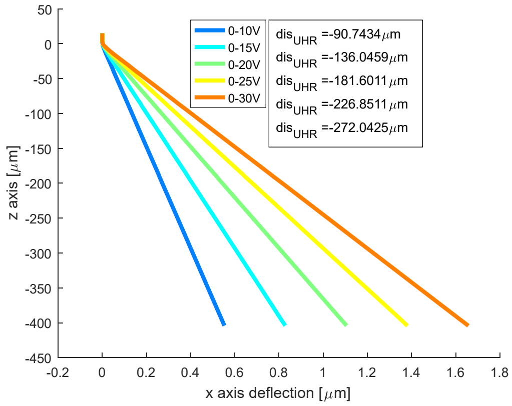

Fig. 33 Particle trajectories (of the central beam) beyond the blanker when the micro deflector (at z=0) is switched on (voltages in the range 10V-30V on one electrode, 0V on the other)

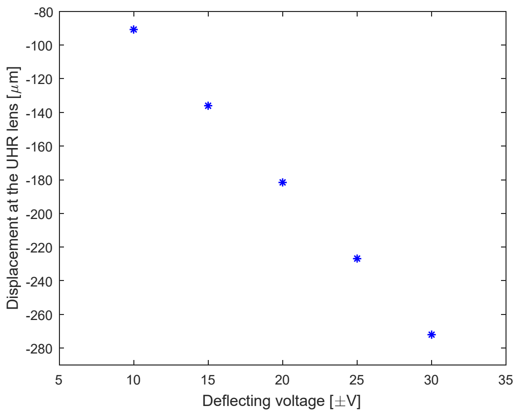

Fig. 34 Deflection of the central beam when the micro blanker is active with the indicated deflecting voltages.

Now the simulation of the combination (Macro + micro deflectors ON) can be done. See figures 35 and 36. A calibration is needed to find out for which settings the angle of the central beam is effectively not changed (it is displaced, but only by a small distance).

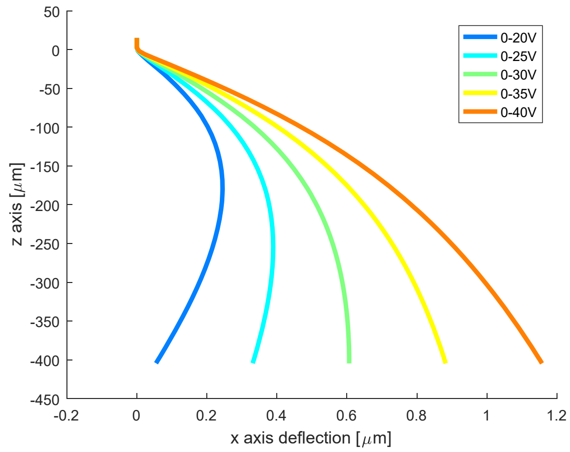

Fig. 35 Macro deflector: -50V -> +50V (symmetric); Micro deflector indicated in legend (asymmetric). When 0V->30V are applied, the beam direction remains vertical.

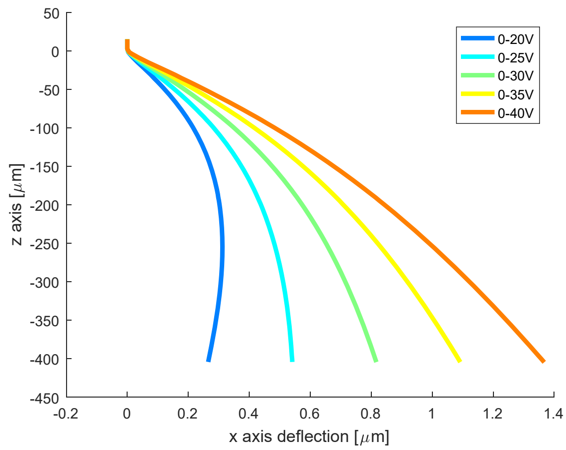

Fig. 36 Macro deflector: -40V -> +40V (symmetric); Micro deflector indicated in legend (asymmetric). When 0V->25V are applied, the beam direction remains vertical.

Fabrication of the blanker plate.

The process steps to fabricate the prototype blanker plate are sketched in figure 37.

To include the blanker plate below the beam splitting optics stack, a complete new stack will be fabricated. All parts are fabricated multiple times, including the stack support structure. The full MBU stack will start with gluing the deflector array plate to the support. We then will align the MLA to the deflector plate, using the alignment tool and alignment markers on both chips. Subsequently the macro electrodes, with insulating spacers, will be aligned to the MLA. Electrical contacts will be made using wire bonding. Special tools are fabricated to hold the support structure fixed and stable during wire bonding. Both sides of the support need bonding, the bottom part for the deflectors, and the top part for the beam splitting optics.

Figure 38 shows an SEM image of the micro deflectors as fabricated already, before the final step of etching the Si handle. Next week (wk 7) we will start stacking and bonding. When the stack passes the electrode voltage tests we will start doing demonstration experiments. When these are successful before the submission deadline of the deliverable report, we will add an addendum that contains the results.

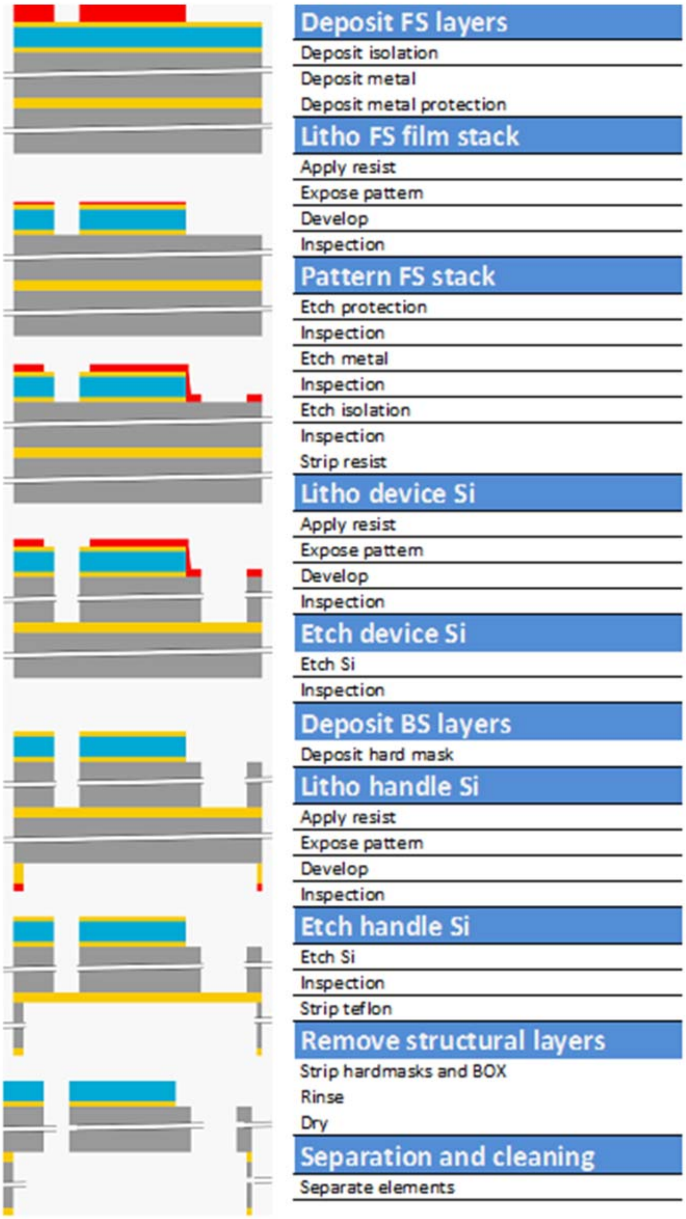

Fig. 37 Process steps to fabricate the blanker array. The colours denote the following: grey: Si, yellow: oxide, blue: metal, red: resist.

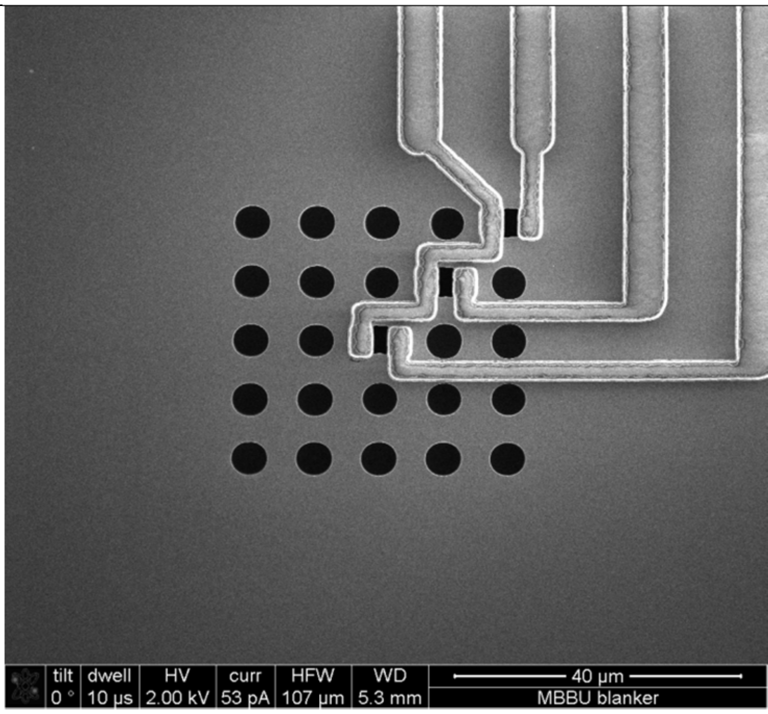

Fig. 38 SEM image of the micro electrodes defined around three of the 25 holes in the deflector array plate. The macro electrodes are at a larger distance from the array, outside of the field of view in the image.

References

[1] A. Mohammadi-Gheidari, C.W. Hagen and P. Kruit, Multibeam scanning electron microscope: Experimental results, J. Vac. Sci. Technol. B28 (2010) C6G5.

[2] A. Mohammadi-Gheidari and P. Kruit, Electron optics of multi-beam scanning electron microscope. Nuclear Instruments and Methods in Physics Research Section A: Accelerators, Spectrometers, Detectors and Associated Equipment 645 (2011) 60-67.

[3] J.E. Barth and P. Kruit, Addition of different contributions to the charged particle probe size. Optik 101 (1996) 101-109

[4] J. Orloff, J. Handbook of charged particle optics, CRC Press, Boca Raton, Florida (1997) 341-389

[5] A.C. Zonnevylle, A versatile tool for sub-micron alignment, stacking and adhesive bonding of electron optical MEMS components, Ch. 5 in 'Individual beam control in multi electron beam systems' by A.C. Zonnevylle, thesis 2017, Delft University of Technology.

[6] A.C. Zonnevylle, R.F.C. Van Tol, N. Liv, A.C. Narvaez, A.P.J. Effting, P. Kruit and J.P. Hoogenboom, Integration of a high-NA light microscope in a scanning electron microscope, Journal of Microscopy 252 (2013) 58-70.

Explanation of Differences between Estimation and Realization	We had some delay in completing the MBU, mainly because of difficulties with the welding of a thin flexible bellows, through which the MBU is to be inserted into the microscope. Extensive vacuum tests had to be done, and a few iterations were needed to get it right. In addition we encountered some delay in the fabrication of the deflector array, as one of the process steps failed, and a different solution had to be found. This caused us to deviate from the tight schedule, explaining why the final tests are not quite done. But we are close and hopefully we can add the results of the final tests before the final submission deadline of the report.
Metrology comments	-